CHAPTER 6

COLOR-MULTIPLEXED OLED DISPLAY ILLUMINATION FOR REALIZATION OF ONE-SHOT MULTI-MODAL MICROSCOPIC IMAGING

This chapter discusses the implication of a cheap and versatile one-shot BF, DF and DPC imaging solution using off-the-shelf optical and electronic components. An effective yet simple illumination engineering has been proposed to generate multiplexed color patterns on an OLED display panel. The OLED panel has been used as an optical source for the realization of one-shot multi-contrast microscopic imaging. This illumination scheme is implemented in both the smartphone microscope and laboratory microscope, and transformed them into multi-contrast imaging platforms for resource-limited areas. Finally, the color channel of the final image recorded by the designed platforms has been decomposed and subsequently computed to obtain the different contrast enhanced imaging of various samples. Both the systems provide three imaging modalities, namely BF, DF, and DPC imaging on a single optical setup.

6.1 Background

Amongst the different modes of imaging that have been discussed in the chapters 3, 4 and 5, BF, DF, and DPC are the most widely used label-free microscopic imaging techniques for studying and quantifying cellular and sub-cellular morphologies with their dynamics [1, 2]. The BF technique is the most basic of them all, where the image contrast is produced due to the variations of optical absorption within the sample. Optically thin or translucent specimens such as living cells do not absorb light significantly without exogenous or endogenous contrast agents. Due to the lack of

intrinsic contrast, the final image is usually very hard to investigate directly under the BF imaging mode. In such cases, other two contrast-enhancing techniques, namely DF and phase-contrast, are more suitable [3, 4]. In DF microscopy, the scattering of the incident beam of light due to the variations in the specimen's refractive index is exploited. It generates rich contrast to most of the unstained thin specimens by employing a hollow cone of light with a larger numerical aperture than the objective lens. Since this specific microscopic technique accentuates the high spatial frequencies associated with the small features in the specimen morphology and structures, it can provide beyond the diffraction-limited resolution in some scenarios. On the other hand, Zernike phase-contrast microscopy generates image contrast by shifting the relative phase of the transparent objects by a quarter wavelengths into the intensity distribution of the final image. This optical phase shift through the phase objects can be considered a powerful endogenous contrast agent since it reveals morphometric features without the need for any exogenous contrast agents like fluorophores. By quantifying the phase value, it also allows to extract of many important biophysical parameters- cell shapes and their dynamics such as growth and kinetics, dry mass and even intracellular refractive index. However, in order to make these contrast-enhancing techniques functional, they require additional optical components, physical masks such as a condenser aperture, conjugate phase ring or annulus, and specialized objective lens. These would eventually increase the overall cost and complexity of the imaging platform exponentially [4]. Moreover, simultaneous image acquisition in the above three imaging modalities on a single optical setup is not possible due to the requirement of additional optical components for each imaging technique.

Researchers, over the years, have proposed and demonstrated many novel contrast-enhancing microscopic techniques to simplify and diversify their applicability by reducing the requirement of extra optical and hardware components. Most of them were based on computationally controllable illumination scheme using an array of LED or coupling a liquid-crystal-display (LCD) as a spatial light modulator (SLM) with the inbuilt optical source of the traditional microscope [2, 5–7]. This has obviated the need of additional design to create a stable phase reference or phase shifting interferometer. DPC microscope has gained attention in the recent years, where partially coherent half-circle illumination is exploited to recover the phase image [8–14]. Efforts have also been made to optimized the above mentioned illumination scheme by introducing radially asymmetric illumination, or gradient amplitude patterns [15].

In this chapter, the adaptation of a tricolor-multiplexed illumination scheme [16] has been designed by using a mini OLED display as a light source and SLM for the realization of cost-effective multimodal microscopic imaging on two different platforms-smartphone and laboratory microscope. These are termed as color-multiplexed smartphone microscope (cmSM) and color-multiplexed laboratory microscope (cmLM), re-

spectively. The color-multiplexed illumination provides the basis for post-processing computation while acquiring the images under BF, DF and DPC in one-shot. In the previously reported works, these imaging modes have been accomplished either using an LED array or integrating an LCD display with the light source of the traditional microscope [4]. However, while using the LED array, since no condenser lens is used, the light collection is not efficient, and only 8-10% of the emitted light from the edge of the LED array can reach the specimen. Again, it is important to calibrate the intensity differences between different LEDs and fluctuations over time. On the other hand, with an LCD as a transparent SLM, it is relatively efficient and easier to acquire different imaging modes. The scheme requires the backlight panel to be removed before using it in the microscopic setup [5]. The inbuilt light source of the microscope illuminates the LCD panel. One of the major drawbacks of this technique is that the LCD has a low extinction ratio, thus will lead to the presence of residue background noise in the captured images [2]. Thus, it is imperative to explore other optical sources and methods to realize multi-contrast imaging at very low-cost and less complexity. Due to the high brightness levels of the commercially available miniature OLED displays as an illumination source, these obstructions can be easily resolved. It provides the most simplest and cost-effective illumination technique, where there is no need of tedious calibration or external light source as in previous cases. The OLED display as a color multiplexed optical source offers three important advantages – (i) it generates perfect spatial patterns as per the needs with very large incident angle, (ii) it is cost-effective, easy to implement, adaptable to any commercial laboratory microscope and smartphone microscope due to small form factor, and (iii) reproduces accurate color with high brightness, which are critical requirements for multimodal imaging using color-multiplexed illumination system.

6.2 Working principle

To realize the multi-contrast microscopic imaging in a single shot, a specific multiplexed color pattern as shown in the figure 6.1 has been employed. Here, a 0.96-inch full color OLED display panel ($7.49) with a pixel resolution of 96 $\times$ 64 has been utilized as a light source to illuminate the specimen. It is highly likely possible that there may be spectral overlapping between the nearest color channels of an RGB color illumination source. This would cause a discrepancy in the final image when computing the color channels to obtain the phase image. To mitigate this issue, the left half-circle of the OLED panel has been set to red (R) and the right half-circle to blue (B), to form the complete circle. The region outside of this circle has been assigned to green channel (G). The radius of the R and B half-circles has been set just greater than the NA of the objective lens of the microscopic system. By maintaining a larger

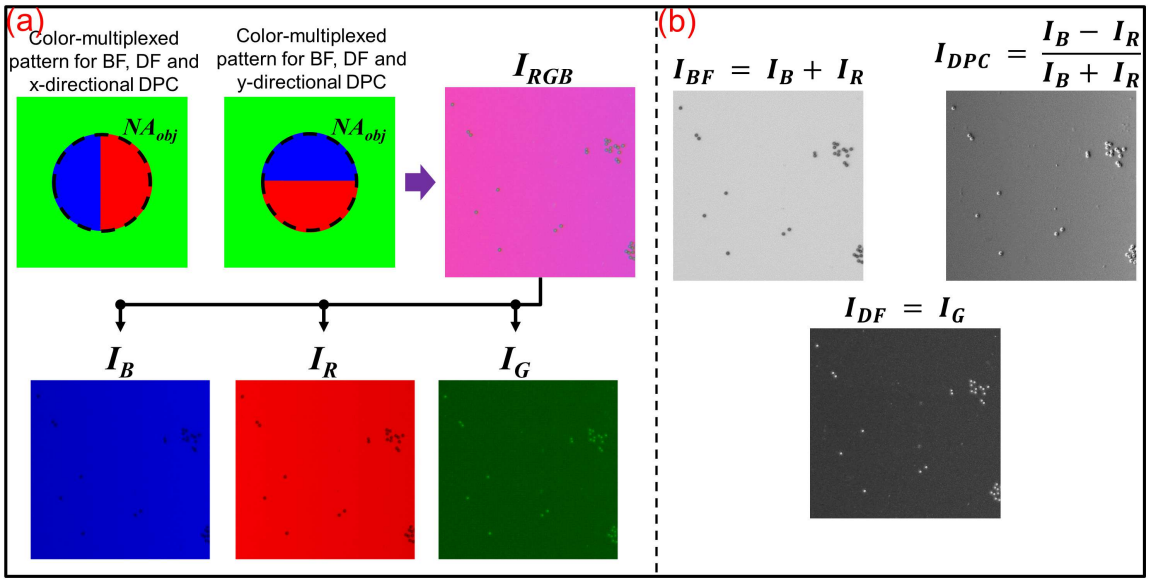

Figure 6.1: Schematic illustration of the color-multiplexed illumination scheme and reconstruction of the respective BF, DF and DPC images.

circular pattern than the NA of the lens, the designed microscopic system will be able to record the phase information in the final image. The G channel will contain the scattered light from the specimen, similar to an oblique illumination system. For the reconstruction of the multi-contrast images, the color channels have been separated into the individual color channels from the final RGB image and computed using the following equations [13]:

$$I_{BF} = I_B + I_R \tag{6.1}$$

$$I_{DF} = I_G \tag{6.2}$$

$$I_{DPC} = \frac{I_B - I_R}{I_B + I_R} \tag{6.3}$$

The summation of the R and B channel will yield the BF image equivalent to the image taken with a full circle. The G channel will produce the DF image, while the ratio of the difference in the intensity level between blue and red channel to its BF mode will constitute the DPC image of the specimen.

6.3 Experimental section

Figures 6.2(a) and 6.2(b) show the optical layout of a $3f$ and $4f$ imaging system implemented to develop the present color-multiplexed imaging systems on smartphone and conventional microscopic platform. The $3f$ system, discussed in chapter 5 has been adapted to construct the cmSM platform. As already unfolded, it consists of

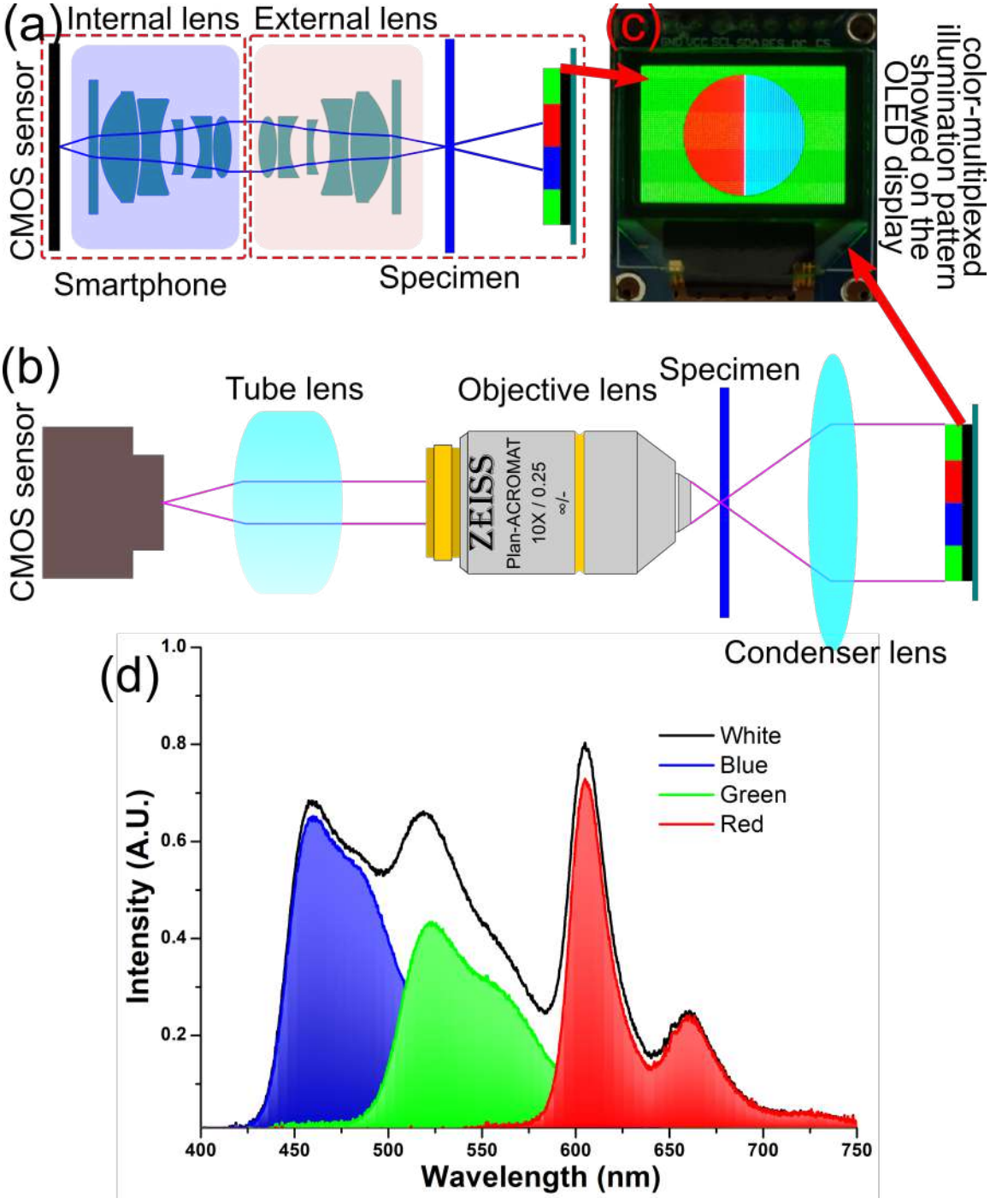

Figure 6.2: Schematic representations of the imaging systems. (a) optical layout of the proposed cmSM system, (b) cmLM setup, (c) photograph of the mini OLED display with the displayed color-multiplexed illumination pattern, and (d) spectral emission profile of the OLED display.

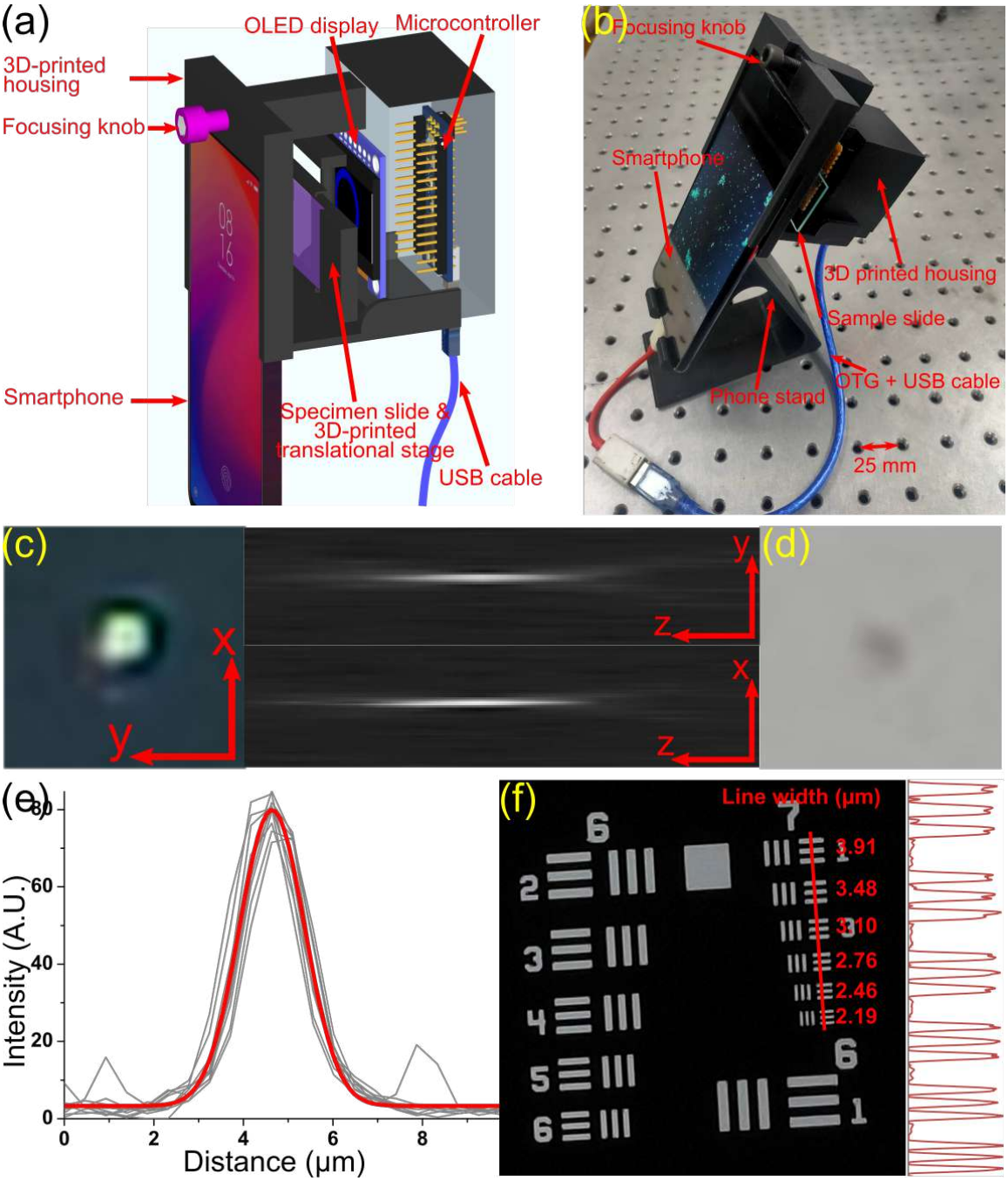

Figure 6.3: Prototype design and characterization of the cmSM system. (a) 3D rendering of the device, (b) developed device attached to a phone, (c) PSF of 1 μm bead in the lateral direction of x-y, y-z and x-z, (d) BF image of the same bead shown in (c), (e) intensity profiles of 10 beads in lateral direction, and (d) imaging of 1951 USAF test target. The intensity profiles of the line elements of group 7 marked in red line is shown on the right side.

an external iPhone 7 front camera lens (FL = 2.87 mm, NA = 0.23, f-number 2.2) as an objective lens and the internal rear camera lens of Redmi K20 smartphone serves as a tube lens. The iPhone 7 front camera lens has been placed in reversed orientation and aligned to the optical axis of the camera lens (FL = 4.77, NA = 0.28, f-number 1.75) of the phone. The Redmi K20 phone has a 48 MP Sony IMX582 CMOS imaging sensor with a pixel pitch of 0.8 μm where four pixels combine to form a single large pixel of 1.6 μm. Considering the pixel pitch of the imaging sensor to be 0.8 μm, the required optical magnification to resolve 1 μm objects is M $\geq$ 1.6 (M $\geq \frac{2\times pixel\ pitch\ of\ the\ sensor}{required\ resolution}$) [17]. This optical setup provides the required optical magnification of 1.6 to resolve 1 μm object by forming a 1:1.6 (object size : image size) finite-conjugated optical system. The motive behind using iPhone camera lens as an objective lens is that it is made of multiple refractive index elements. Thus, possible aberrations and distortions in the final image have been eliminated by using this lens as an objective, which is otherwise may present with the other conventional optical lenses. The miniature full color OLED display panel has been placed at a distance of 15 mm from the specimen plane for illumination and is shown in figure 6.2(c). The color reproducibility of the OLED display has been initially studied using a CCD spectrometer (CCS200, Thorlabs). Figure 6.2(d) shows the characteristic spectral response of the spectrometer when the OLED panel is illuminated with white and the other three primary colors. The display panel has been controlled and powered by Arduino Nano microcontroller board. Serial communication has been established between the microcontroller and an openly available smartphone application, 'Serial USB Terminal' to control the display by the phone via USB-OTG protocol. The smartphone battery provides the required power to operate the microcontroller (operating voltage 5V). The prototype of the cmSM has been built using 3D printer and is shown in figure 6.3(a) and (b). All the optical and electronic components were rigidly mounted within the 3D-printed housing. A 3D-printed translational stage with a sample holder has also been incorporated into the designed cmSM system to ease the specimen's movement in x and y-direction and focus in the z-direction.

A basic laboratory microscope (Carl Zeiss Primo Star) that is capable of imaging only in BF mode has been considered to develop the proposed cmLM system. The microscope is equipped with a 5 MP Axiocam 105 color camera having a pixel pitch of 2.2 μm. To convert it into cmLM for multimodal, multi-contrast imaging, the inbuilt optical source has been replaced with the OLED display module. The OLED panel has been placed at a distance of 95 mm from the specimen plane. To obtain the optimal illumination of the specimen, the condenser lens has been readjusted. Figure 6.1(b) shows the schematic representation of the proposed cmLM system. Similar to the cmSM system, the illumination pattern of the OLED panel has been controlled by the same technique. For parallel comparison of the performance between cmSM

and cmLM systems, the 10×/0.25NA objective lens of the laboratory microscope has been considered.

6.4 Optical characterization of the cmSM system

The optical magnification (M) of the cmSM system which is the ratio of the focal lengths of the phone's internal lens (FL = 4.77 mm) to the external lens (FL = 2.87 mm), is found to be 1.66×. The phone has a screen size of 6.39 inch (diagonal) with an aspect ratio of 19.5:9. The unzoomed image will have a digital magnification ($M_d = \frac{Screen\ size}{Sensor\ size}$) of 20.3× when displayed on the phone screen. The NA of the objective lens of the cmSM is 0.23. This gives a maximum theoretical diffraction-limited resolution of 1.45 μm ($R_{diff} = \frac{0.61\lambda}{NA}$, λ = 550 nm). Again, the point spread function (PSF) of the cmSM system has been evaluated at varying depths in DF mode by imaging 1 μm beads. Figure 6.3(c) represents the PSF in x-y, y-z and x-z directions. The measurement of FWHM of the PSFs of 10 different beads in lateral direction is shown in figure 6.3(e). The bold red curve represents the Gaussian-fitted average intensity distribution of the beads which shows the experimental FWHM value of 1.25 μm. The BF mode imaging of the 1 μm bead captured by the cmSM system is also shown in figure 6.3(d). Figure 6.3(f) clearly shows that the cmSM system can spatially resolve the highest line element of the 1951 USAF resolution test target (width 2.19 μm) with ease. The field of view (FoV) of the system is characterized to be 3.1 mm^2. Considering the FWHM resolution of 1.25 μm of the cmSM system, the space-bandwidth product ($SBP = \frac{field\ of\ view}{(0.5\times r)^2}$, where r = resolution) is calculated to be ∼8 megapixels. This means that the proposed system could be effective for high throughput imaging applications where a large FoV with high resolution is indispensable.

6.5 Algorithm to construct the multi-contrast microscopic images

After constructing the imaging systems, an algorithm has been developed on the Matlab mobile platform to reconstruct the one-shot multi-contrast images within the phone itself. Figure 6.4 illustrates the pictorial representation of the reconstruction algorithm to obtain BF, DF and DPC images. At first, the script of the algorithm is uploaded on the MathWork's server and accessed on the Matlab mobile platform as shown in the figure 6.4(a) and (b). After running the script, the results can be visualized in figure 6.4(c)-(g). The reconstructed BF, DF and DPC images can be seen in figure 6.4(h)-(j), respectively.

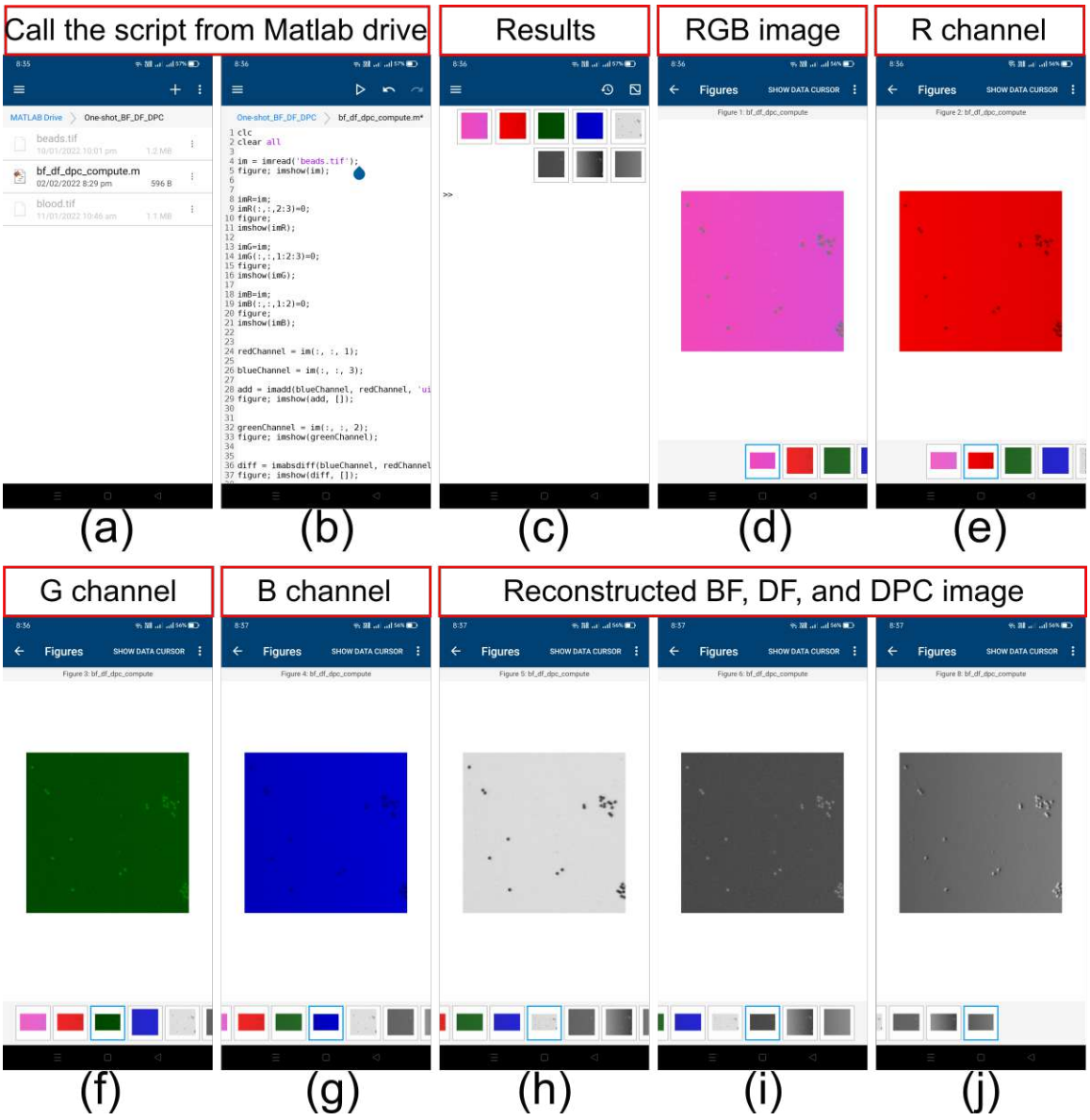

Figure 6.4: Graphical representation of the algorithm to reconstruct the multi-contrast BF, DF and DPC images on Matlab mobile platform.

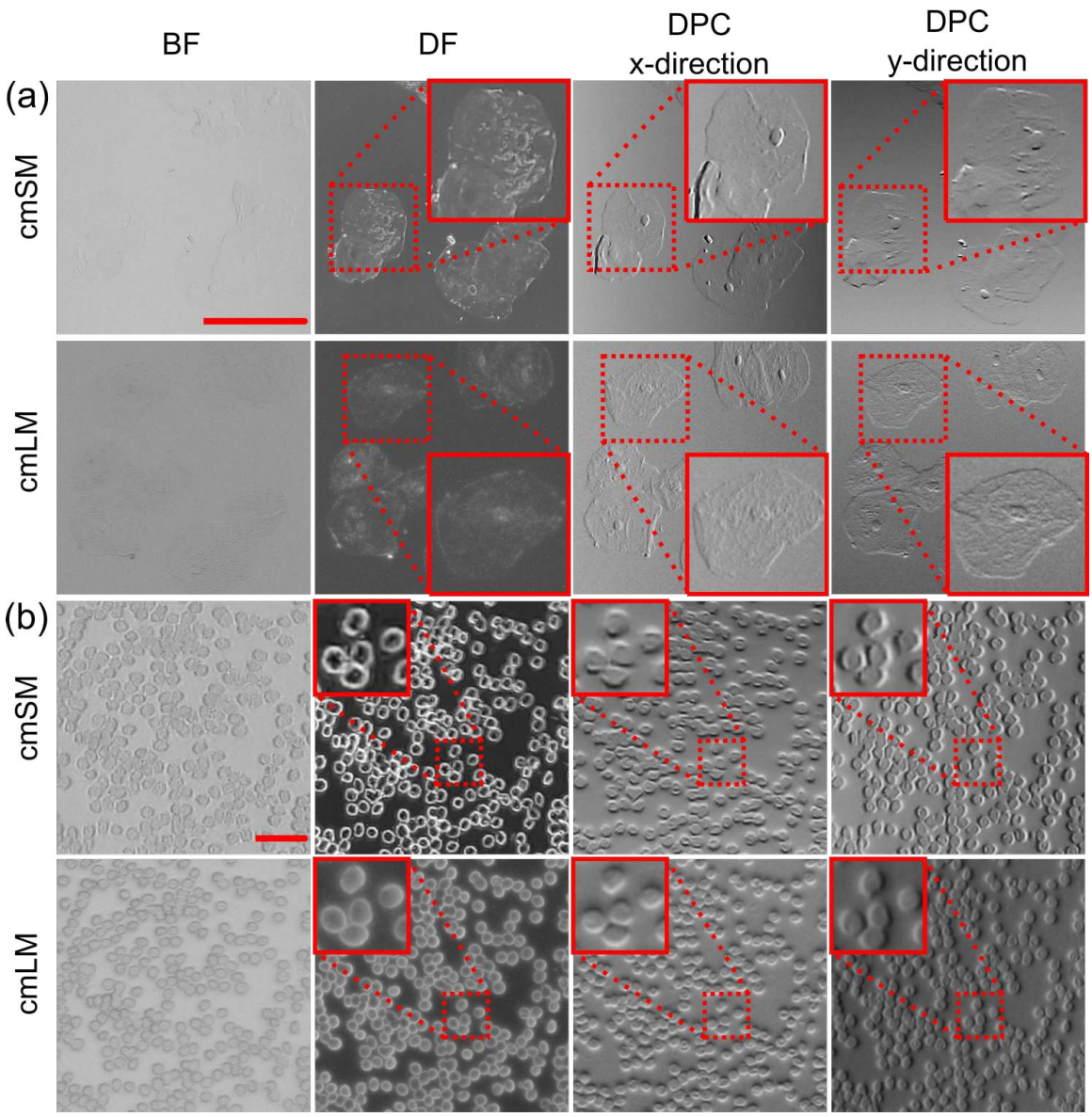

Figure 6.5: Imaging of biological unstained specimens with the proposed microscopic systems. (a) HECC cells captured in BF, DF, and DPC (x and y-direction) with cmSM and cmLM respectively, (b) human blood under BF, DF, and DPC (x and y-direction) captured using the both systems respectively. Scale bars are 20 μm.

6.6 Practical applications of the proposed systems

To demonstrate the ability of the proposed system to capture multiplexed, multi-contrast imaging in one-shot, two unstained biological specimens-HECC and human blood samples have been considered for imaging with both cmSM and cmLM system. Their performance has been compared in terms of contrast ($C = \frac{I_{max}-I_{min}}{I_{max}+I_{min}}$, I_{max} is the maximum intensity of the specimen and I_{min} is the minimum intensity of the background) and SNR ($SNR = \frac{I_{specimen}-I_{bg}}{\sigma_{bg}}$, $I_{specimen}$ is the average intensity of the specimen, I_{bg} is the average intensity of the background and σ_{bg} is the standard deviation of the background). Finally, the color-multiplexed one-shot DPC imaging of hyphae formation of *C. albicans* has been demonstrated. Figure 6.5 represents the corresponding one-shot BF, DF and DPC modes imaging of the specimens. Unstained HECC cells are translucent in nature. Thus, the BF image does not produce sufficient contrast (C = 0.016 and 0.012 respectively) to view with both the imaging systems. However, in DF (C = 0.14 and 0.13 respectively) and DPC modes (C = 0.03 and 0.04 respectively) the cells are clearly visible with both the systems. DPC images provide better visualization in terms of microstructures which are not visible in either BF or DF imaging mode. Similarly, unstained blood sample has been imaged with both the cmSM and cmLM systems. For cmSM system, the contrast and SNR values in BF, DF and DPC modes are found to be (0.05, 7.29), (0.49, 56.9), and (0.048, 6.1) respectively. In case of cmLM, the contrast and SNR values of the considered imaging modes are (0.06, 8.45), (0.4, 17.36,) and (0.06, 5.77) respectively. As expected, an enhanced contrasts and SNR values have been noticed for DF and DPC modes compared to BF mode of imaging. The contrast and SNR values in cmSM system are observed to be better than the cmLM system. However, the cell morphology and its microstructures features of the samples in cmLM system are seen clearer than the cmSM system. For clarity, the inset in figures 6.5(a) and (b) show the zoomed-in view of DF and DPC modes of the considered biological samples acquired by both the imaging platforms. Finally, the applicability of the smartphone based DPC microscope has been demonstrated by imaging one of the *Candida* species fungus-*C. albicans*. *Candidiasis* is a fungal infection in human body caused by this *Candida* species. Imaging of this fungus specimens using the proposed cmSM system could demonstrate the proficiency and usability of the device for diagnostics applications at PoC level. Figure 6.6(a) depicts the one-shot qualitative DPC imaging of *C. albicans* without staining. The hyphae formations of the cells can be seen clearly in the DPC mode. The ROI marked in red square in figure 6.6(a) has been enlarged in figure 6.6(b). For comparison, the same ROI has been provided in figures 6.6(c) and (d) that have been acquired under BF and DF imaging modes. These figures clearly reveal that the BF and DF mode of imaging do not produce sufficient contrast to

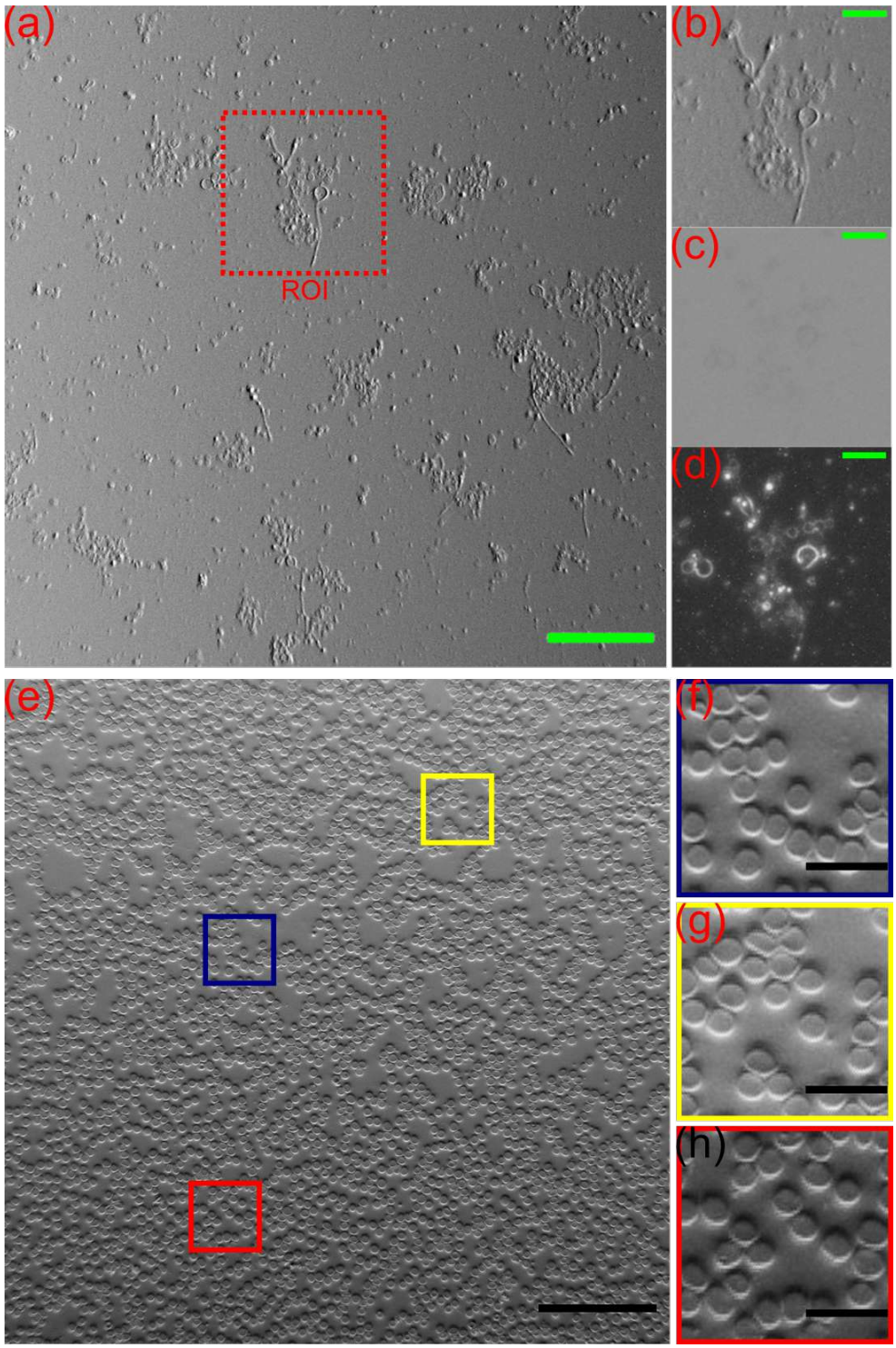

Figure 6.6: Applications of color-multiplexed DPC imaging of the cmSM system for biomedical imaging. (a) One-shot DPC imaging of hyphae formation of *C. albicans* without staining. Scale bar is 100 μm. (b), (c) and (d) the enlarged view of the ROI indicated in red square in (a), corresponding BF and DF images of the same ROI respectively. Scale bars are 20 μm. (e) DPC image of unstained human blood smear captured using the proposed smartphone multi-contrast system. Scale bar is 100 μm. (f), (g) and (h) are the enlarged regions marked in (e) respectively. Scale bars are 20 μm.

view this specific sample compared to DPC mode. A large FoV of captured blood cells are also included in the figure 6.6(e). The cell boundaries and morphologies are clearly visible under DPC mode which can be seen from the enlarged view as shown in figures 6.6(f), (g) and (h). In this report, only the qualitative DPC imaging has been performed, as the primary emphasis is to demonstrate low-cost multimodal multi-contrast imaging device in one-shot from the samples.

Again, from the figure 6.5, one can clearly observe that the cmLM outperforms the cmSM which is obvious due to its costly optical and electronic components. However, cmSM has many advantages in terms of cost and size. The net cost involved to develop of the cmSM system excluding the smartphone is only $25.7, whereas the cost involved of the laboratory microscope is ∼$2000). Due to its small size (80 mm × 45 mm × 45 mm) and weight (∼96 gm), the cmSM can be used for in-field applications. It is important to mention here that the actual resolution of the cmSM system is pixel-limited. The resolution is, further, affected by the presence of the Bayer color filter over the CMOS sensor of the phone. Image compression algorithm of the phone further reduces the resolution of the cmSM system. Even though, the resolution of the cmSM device is estimated to be 1.25 μm experimentally with a very wide FoV area. Considering the minimal development cost, and high SBP value of the cmSM, it is envisioned that the present system could emerge as a potential alternative multimodal imaging platform in the near future.

6.7 Discussion

The use of a miniature OLED display in the cmSM system for controllable multiplexed illumination offers several advantages over the previously reported LED array-based smartphone multi-contrast microscope [18]. The illumination optics of the cmSM system can be powered and controlled from the phone itself, thus obviating the need of external power supply. The consumption of power of the OLED panel (∼20mA at 3.3V) is less compared to an LED array. This implies a longer period of operation of the designed microscopic system compared to the LED array-based multi-contrast imaging. The objective lens of a smartphone microscope might be required to replace with another different kind of objective lens as per the need. In such a case, if the LED array is not properly positioned and calibrated, the final results might be distorted. For example - with a phone camera lens as an objective lens and a LED array illumination, the system might suffer many discrepancies in the final image if special care is not taken [19]. This kind of complication is not observed in our cmSM system. Any miniature objective lens such as an achromatic doublet or singlet lens can be used in place of the external phone camera lens since the NA of the illumination pattern on the OLED display panel can be easily adjusted dynamically.

Again, because of the densely-packed organic pixels, the OLED display panel can generate much complicated illumination patterns with accurate color compared to an LED array which gives an edge to the cmSM system that enable us to design new microscopic tools. Additionally, due to the small form factor of the OLED display, it is also possible to integrate it into any regular microscope without any mechanical modifications enabling inexpensive multi-contrast imaging.

6.8 Summary

In summary, the chapter discusses a simple, rapid and relatively low-cost technique to acquire multimodal multi-contrast imaging on a smartphone and laboratory microscope. Imaging of unstained biological samples under BF, DF and DPC modes have been reliably acquired by both the systems. The use of OLED display to generate multiplexed color patterns is relatively simple and can be implemented on any smartphone and laboratory microscope. It also offers a large degree of freedom to create other illumination patterns suitable for other contrast enhancing imaging modalities such as multi-color fluorescence, polarization, oblique illumination, and Rheinberg mode of imaging without any further modifications, as in the case of LCD panel or LED array. This will increase the functionality and applicability of the technique for other applications. With the proposed illumination scheme, the dynamical behaviors of biological specimens can also be monitored in a one-shot under multi-contrast mode not only with a laboratory microscope but also on a smartphone.

References

[1] Murphy, D. B. *Fundamentals of light microscopy and electronic imaging*. John Wiley & Sons, 2002.

[2] Guo, K., Bian, Z., Dong, S., Nanda, P., Wang, Y. M., and Zheng, G. Microscopy illumination engineering using a low-cost liquid crystal display. *Biomedical optics express*, 6(2):574–579, 2015.

[3] Popescu, G., Ikeda, T., Dasari, R. R., and Feld, M. S. Diffraction phase microscopy for quantifying cell structure and dynamics. *Optics letters*, 31(6):775–777, 2006.

[4] Park, Y., Depeursinge, C., and Popescu, G. Quantitative phase imaging in biomedicine. *Nature photonics*, 12(10):578–589, 2018.

[5] Zuo, C., Sun, J., Feng, S., Hu, Y., and Chen, Q. Programmable colored illumination microscopy (pcim): a practical and flexible optical staining approach for

microscopic contrast enhancement. *Optics and Lasers in Engineering*, 78:35–47, 2016.

[6] Ogasawara, Y., Sugimoto, R., Maruyama, R., Arimoto, H., Tamada, Y., and Watanabe, W. Mobile-phone-based rheinberg microscope with a light-emitting diode array. *Journal of biomedical optics*, 24(3):031007, 2018.

[7] Drexler, W., Liu, M., Kumar, A., Kamali, T., Unterhuber, A., and Leitgeb, R. A. Optical coherence tomography today: speed, contrast, and multimodality. *Journal of biomedical optics*, 19(7):071412, 2014.

[8] Lin, Y.-Z., Huang, K.-Y., and Luo, Y. Quantitative differential phase contrast imaging at high resolution with radially asymmetric illumination. *Optics letters*, 43(12):2973–2976, 2018.

[9] Suzuki, Y., Odaira, M., Ohde, H., and Kawata, Y. Quantitative phase imaging by optimized asymmetric illumination. *Applied Optics*, 56(25):7237–7242, 2017.

[10] Chen, M., Phillips, Z. F., and Waller, L. Quantitative differential phase contrast (dpc) microscopy with computational aberration correction. *Optics Express*, 26 (25):32888–32899, 2018.

[11] Mehta, S. B. and Sheppard, C. J. Quantitative phase-gradient imaging at high resolution with asymmetric illumination-based differential phase contrast. *Optics letters*, 34(13):1924–1926, 2009.

[12] Kheireddine, S., Smith, Z. J., Nicolau, D. V., and Wachsmann-Hogiu, S. Simple adaptive mobile phone screen illumination for dual phone differential phase contrast (dpdpc) microscopy. *Biomedical optics express*, 10(9):4369–4380, 2019.

[13] Phillips, Z. F., D'Ambrosio, M. V., Tian, L., Rulison, J. J., Patel, H. S., Sadras, N., Gande, A. V., Switz, N. A., Fletcher, D. A., and Waller, L. Multi-contrast imaging and digital refocusing on a mobile microscope with a domed led array. *PloS one*, 10(5):e0124938, 2015.

[14] Tian, L. and Waller, L. Quantitative differential phase contrast imaging in an led array microscope. *Optics express*, 23(9):11394–11403, 2015.

[15] Fan, Y., Sun, J., Chen, Q., Pan, X., Trusiak, M., and Zuo, C. Single-shot isotropic quantitative phase microscopy based on color-multiplexed differential phase contrast. *APL Photonics*, 4(12):121301, 2019.

[16] Lee, D., Ryu, S., Kim, U., Jung, D., and Joo, C. Color-coded led microscopy for multi-contrast and quantitative phase-gradient imaging. *Biomedical optics express*, 6(12):4912–4922, 2015.

[17] Agbana, T. E., Diehl, J.-C., van Pul, F., Khan, S. M., Patlan, V., Verhaegen, M., and Vdovin, G. Imaging & identification of malaria parasites using cellphone microscope with a ball lens. *PloS one*, 13(10):e0205020, 2018.

[18] Jung, D., Choi, J.-H., Kim, S., Ryu, S., Lee, W., Lee, J.-S., and Joo, C. Smartphone-based multi-contrast microscope using color-multiplexed illumination. *Scientific reports*, 7(1):1–10, 2017.

[19] Switz, N. A., D'Ambrosio, M. V., and Fletcher, D. A. Low-cost mobile phone microscopy with a reversed mobile phone camera lens. *PloS one*, 9(5):e95330, 2014.